Impacts of glass homogenization on optical properties of rare-earth ion doped chalcogenide glass

S. W. Xu[a,*], X. N. Yang[a], J. H. Yang[a], R. X. Wang[a], X. Q. Su[b]
aCollege of Mathematics and Physics, Hunan University of Arts and Science, 415000, Changde, People's Republic of China
bCollege of Applied Sciences, Beijing University of Technology, 100124, Beijing, People's Republic of China

In rare-earth ion doped chalcogenide glass, the impacts of glass homogenization on optical properties were studied in this work. A series of $Ge_{24}Ga_{10}Se_{65}:Er_1$ glasses were fabricated by melt-quenching method under the same condition with different melting time. The structure of the obtained glasses was characterized, absorption and emission spectra were recorded, and lifetime of the $^4I_{13/2}$ state of Er^{3+} ions was measured as well. It is found that the melting time does not have obvious influence on glass structure, absorption and emission properties of erbium ions. A significant improvement on lifetime was noticed with the increase of melting time.

1. Introduction

Light sources and amplifiers operating in the mid-infrared (MIR) wavelength have attracted many attentions due to their wide applications in the field of supercontinuum generation, chemical sensing, medical laser surgery, and environmental monitoring [1-6]. Currently, MIR sources include globar, quantum cascade laser (QCL), optical parametric oscillator/amplifier (OPO and OPA), and transition metal doped polycrystalline chalcogenide. However, each has their own disadvantages. For example, low brightness limits globar's performance in high spatial resolution applications; QCL has enough brightness in some wavelength band but is quite costly and complex; for OPA/OPO, tight constrains apply on the excitation source, which requires narrow linewidth and linear polarized excitation sources [7]; and thermal management becomes a challenge when higher power output is required for transition metal doped ZnSe/ZeS [8].

Properties chalcogenide glasses possess, such as wide optical transparency window, high refractive indices, low phonon energy (~350 cm^{-1} for sulfides, ~250 cm^{-1} for selenides and 200 cm^{-1} for tellurides) which could reduce the non-radiative multiphonon relaxation rate significantly, and reasonable rare-earth doped concentration in Ga-containing chalcogenide glasses [9, 10], making it perfect host material for rare-earth ions in light amplification and lasing applications. Therefore, rare-earth ions doped chalcogenide glasses are thought promising candidates in realizing emissions in near and mid-infrared.

Chalcogenide glasses are normally synthesized by melt-quenching method. In this method, mixed raw elements are sealed in a vacuumed ampoule. The mixtures is then melted at high temperature, and keep at this temperature for a certain period of time (from hours to days) for a homogeneous melting, followed by air or cooled water quenching to form the glass. It is thought that keep the mixture at melting temperatures for 24 hours with a continuous rocking, melt homogeneity could be achieved. However, R. Bhageria pointed out in Ge-Se system, the structure and physical properties of the glass was evolved with melting time and eventually reach its homogeneity state after a long time depending on glass composition, for example 6 days for

$Ge_{10}Se_{90}$, and 17 days for $Ge_{15}Se_{85}$ [11]. In rare-earth ion doped chalcogenide glass, the properties of host glass and the uniform distribution of rare-earth ions in host matrix are critical for photoluminescence (PL). Although chalcogenide glasses doped with different rare-earth ions, such as Er^{3+}, Dy^{3+}, Tm^{3+}, Tb^{3+} and Ho^{3+}, were extensively studied [12-19] and great progress has been made, the impacts of melting time on the emission properties of rare-earth ion are not been fully investigated.

In this paper, erbium doped chalcogenide glasses (Ge-Ga-Se) are synthesis by using melt-quenching method. Three samples of the same composition and erbium doped concentration were fabricated with same procedure, except different melting time. Samples are characterized with Raman spectra, absorption spectra, photoluminescence and PL lifetime. The impacts of melting time on erbium ion emission properties were investigated carefully and discussed based on the results.

2. Experimental

Bulk Ge-Ga-Se samples were prepared by melt-quenching technique. The composition $Ge_{24}Ga_{10}Se_{65}$:Er_1 was chosen as it is stoichiometry which promises stable properties in the glass, and the 10 at% of gallium containing in this composition will ensure at least 1 at% of erbium ions could be kept in the glass matrix without clustered [20]. All the raw materials used are high purity (5N). the required amount of raw materials was weighed in a glove box flashed with dry nitrogen, and then loaded in quartz ampoule. The quartz ampoule was pumped down and then sealed with oxygen-hydrogen torch when the pressure reached $\sim 10^{-6}$ Torr. Then the sealed ampoules were transferred into a rocking furnace, and melted at 950 °C for 12 hours, 42 hours and 65 hours respectively. After melting, the ampoules were removed form furnace and quenched in cold water, following 2 hours annealing at 375 °C, which is 20 °C lower than the T_g of this composition, and then cooled down to room temperature slowly. The obtained glass rods were cut into small pieces of ~ 3 mm thickness and both sides polished for the following characterizations.

Raman spectra of the glasses were recorded at room temperature using a laser confocal Raman spectrometer (Renishaw inVia, Gloucestershire, UK) with an excitation at 630 nm. In Raman measurement, the excitation power was kept low as ~ 1mW to avoid any photo-induced effects. Absorption spectra of the three $Ge_{24}Ga_{10}Se_{65}$:Er_1 bulk glasses were recorded using a Cary 5000 UV-Vis-NIR spectrophotometer. The photoluminescence (PL) spectra of the glasses were collected using a Horiba Jobin Yvon 64000 spectrometer. The excitation laser operated at 830 nm, and an InGaAs detector cooled with liquid nitrogen was used to record the spectrum from 1480 nm to 1600 nm. The photoluminescence decay curve of transition between $^4I_{13/2}$-$^4I_{15/2}$ states of Er^{3+} ions was experimentally recorded with an excitation wavelength of 1490 nm, and then the fluorescence lifetime was extracted by fitting the decay curve with a single exponential function.

3. Results and discussion

Raman spectra of the three samples of the same composition but different melting time were measured and shown in Fig. 1. All the spectra are normalized and offset vertically for comparison. The Raman spectrum contains two main features: one strong peak at 204 cm^{-1} with two shoulders at 177 cm^{-1} and 216 cm^{-1}; and a broad low-intensity band ranging from 230 cm^{-1} to 330 cm^{-1}. The strong peak at 204 cm^{-1} is associated with the $\nu_1(A_1)$ symmetric stretching modes of corner-sharing [GeSe$_{4/2}$] tetrahedra. The left shoulder at 177 cm^{-1} is thought related with the stretching modes of Ge-Ge, Ga-Ga or Ge-Ga bonds (A$_G$ vibration modes) in $Ge_2Se_{6/2}$, $Ga_2Se_{6/2}$ or $GeGaSe_{6/2}$ structural units [21]. The right-side shoulder at 216 cm^{-1} is assigned to the vibration of edge-shared bi-tetrahedral $Ge_2Se_{8/2}$ units [22]. The broad band from 230 cm^{-1} to 330 cm^{-1} is a result of multi-band combination, which includes the vibration of Se-Se bonds (245 cm^{-1} and 265 cm^{-1}), and vibration of GeSe$_4$ structural units (300 cm^{-1}). Also, it is well known that in Ge-Ga-Se glass, the atomic weight of Ge and Ga atom, and bond strength of [Ge-Se$_4$] and [Ga-Se$_4$], are similar to each other [21], thus the Raman band of Ge-containing structural units and Ga-

containing structural units are likely to overlap with each other, adding difficulty in distinguishing them.
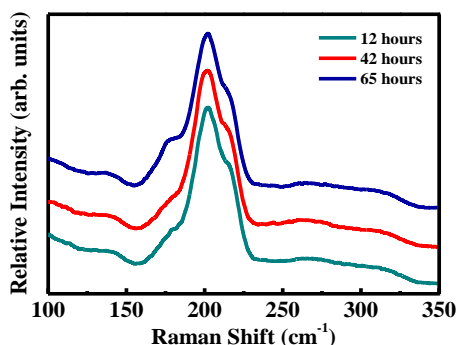

Fig. 1. Normalized Raman spectra of the three samples with different melting time.

Except the intensity of the band at 177 cm^{-1} in the 65-hour melting sample is stronger than other two samples, no significant difference is noticed from the spectrum. Strong band at 177 cm^{-1} refers to the Ge-Ge and/or Ga-Ga bond concentration is high in this sample, however, the reason for this sudden change needs further investigation. Also, with 1 at% of erbium ion, there is almost no sign of erbium related bond shown in the spectrum, which is consistent with the reports in ref [23], in which they claim that the introduce of a small amount of rare-earth into the glass matrix normally only results in minor change in glass structure.
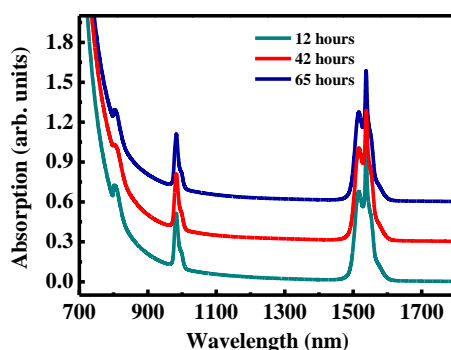

Fig. 2. Normalized absorption spectra of the three samples with different melting time.

The normalized absorption spectra from the 3 mm thick samples are shown in Fig. 2. The strongest band locates at 1538 nm arises from the transition $^4I_{15/2}$-$^4I_{13/2}$ of erbium ions. While the peaks at 985 nm and 809 nm correspond to the $^4I_{15/2}$-$^4I_{11/2}$ and $^4I_{15/2}$-$^4I_{9/2}$ transitions, respectively. The significant increase of absorption around 800 nm indicates the existence of weak absorption tail, and the absorption increases in an exponential way at even shorter wavelength as it reaches its bandgap wavelength. The peak position of the three samples are identical, and a small absorption peak intensity variation was noticed but locates in the range of measurement error.

The obtained emission spectra from three samples were normalized to have the same peak value around 1538 nm, and were shown in Fig. 3. Emissions from three samples with different melting times have the very similar line shape and band position, which locates at 1538 nm corresponding to the radiative decay between $^4I_{13/2}$-$^4I_{15/2}$ states of erbium ions. The peak emission wavelength 1538 nm is red-shifted compared with the same emission in oxide glass host (for example 1533 nm in Er:Al$_2$O$_3$ [24], 1535 nm in Er:SiO$_2$ [25]). This red-shift is thought caused by the nephel-auxetic effect (electron cloud expanding), that is radiative absorption and emission of rare-earth ions tend to red-shift in a more covalent lattice [26].
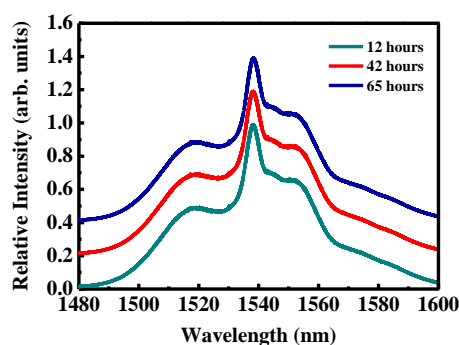
Fig. 3. Normalized PL spectra of the three samples with different melting time.

Since all the samples are doped with the same amount of erbium, fabricated followed the same procedure, and measured under the same condition, it is possible to compare the absolute emission intensity of the peak value from the emission spectra. After background noise removal, the peak emission intensity at 1538 nm were extracted from each spectrum and plotted in Fig. 4. The intensity fluctuated from sample to sample, but only in a 7% range. This variation may arise from the sample emission itself, but other factors, such as parallelism of sample surface, polish quality, and alignment in each spectrum measurement, could also contribute to this variation. Therefore, it is hard to conclude that the melting time has a significant impact on the emission intensity in this set of samples from Fig. 4.
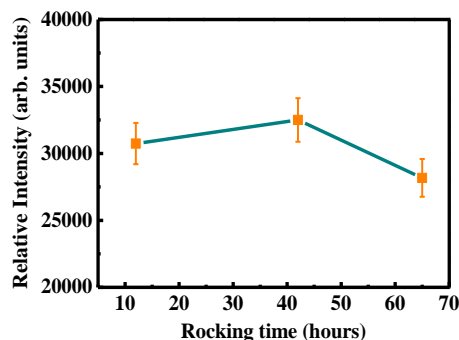

Fig. 4. PL intensity at 1538 nm of the three samples with different melting time.

Lifetime of the $^4I_{13/2}$ state of Er^{3+} ions from the three samples with different melting time was shown in Fig. 5. From the result, the 12-hour melting sample has the shortest lifetime of 1.12 ms, while the longest lifetime 1.35 ms was found from the 65-hour melting sample, and in the middle 1.27 ms was achieved in the 42-hour melting sample. The error of this lifetime measurement is about 3%. The trend of the improvement in lifetime is obvious. With the increase of melting time, the lifetime of erbium ion at $^4I_{13/2}$ state gets increased with a slop of 0.0044 ms/hour. This could be explained in the following ways. On one hand, with long melting time the Ge-Ga-Se glass matrix get well bonded and become more homogeneous, which offers a better host glass matrix for erbium ions. However, this small matrix structure change was not picked up in Raman spectrum we obtained. On the other hand, the rare-earth ions may also distribute more uniformly and bonded properly with Se atoms in the matrix [27]. It is well known that the ion-ion interaction process, such as energy transfer and up-conversion process, can significantly shorten the lifetime due to the too close physical distance of ions [28]. Even in a low erbium ion concentration sample, if the erbium ion is not evenly distributed, local ion-ion interaction could also happen due to the short local ion-ion distance, which in turn will shorten the lifetime. Obviously, long melting time in glass fabrication can reduce this local ion-ion interaction process,

and therefore offer a longer lifetime. It is also expected a PL intensity enhancement in long melting time sample, unfortunately, it was not shown from the result in Fig. 4.
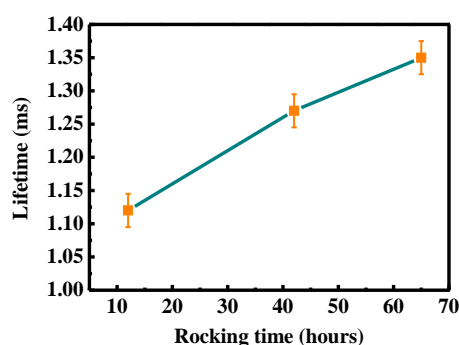

Fig. 5. Lifetime of the $^4I_{13/2}$ state of Er^{3+} ions from the three samples with different melting time.

4. Conclusions

Three identical erbium doped $Ge_{24}Ga_{10}Se_{65}:Er_1$ samples with different melting time were fabricated. In these samples, no structure change was observed in Raman spectra. Both absorption and emission spectra show similar features with only minor variation in peak intensity. Lifetime of the $^4I_{13/2}$ state of Er^{3+} ions increased from 1.12 ms to 1.35 ms with the increment of melting hours, implying a more homogeneous chalcogenide host and a better distribution of erbium ions in the glass matrix, which benefit its application as active chalcogenide glasses.

References

[1] Y. Yu, X. Gai, P. Ma, D. Y. Choi, Z. Y. Yang, R. P. Wang, S. Debbarma, S. J. Madden, B. Luther-Davies, Laser Photonics Rev. **8**, 792 (2014).
[2] R. Chahal, F. Starecki, C. Boussard-Pledel, J. L. Doualan, K. Michel, L. Brilland, A. Braud, P. Camy, B. Bureau, V. Nazabal, Sens. Actuators B Chem. **229**, 209 (2016).
[3] S. N. Nam, V. Fedorov, S. Mirov, K. H. Hong, Opt. Express **28**(22), 32403 (2020).
[4] F. Starecki, F. Charpentier, J. L. Doualan, L. Quetel, K. Michel, R. Chahal, J. Troles, B. Bureau, A. Braud, P. Camy, V. Moizan, V. Nazabal, Sens. Actuators B Chem. **207**, 518 (2015).
[5] S. Gu, N. Zhang, Q. Zhang, R. Pan, Chalcogenide Lett. **12**(5), 257 (2015).
[6] M. Essi, G. Cisse, V. Flaud, Chalcogenide Lett. **17**(10), 495 (2020).
[7] Y. H. Shen, S. U. Alam, K. K. Chen, D. J. Lin, S. S. Cai, B. Wu, P. P. Jiang, A. Malinowski, D. J. Richardson, IEEE J. Sel. Top. Quant. **15**, 385 (2009).
[8] S. D. Jackson, Nat. Photonics **6**, 423 (2012).
[9] T. W. Allen, M. M. Hawkeye, C. J. Haugen, R. G. DeCorby, J. N. McMullin, D. Tonchev, K. Koughia, S. O. Kasap, J. Vac. Sci. Technol. A **22**, 921 (2004).
[10] D. T. Tonchev, C. J. Haugen, R. G. DeCorby, J. N. McMullin, S. O. Kasap, J. Non-Cryst.

Solids **326**, 364 (2003).

[11] R. Bhageria, K. Gunasekera, P. Boolchand, M. Micoulaut, Phys. Status Solidi B **251**, 1322 (2014).

[12] B. J. Park, H. S. Seo, J. T. Ahn, Y. G. Choi, J. Heo, W. J. Chung, J. Ceram. Soc. Jpn. **116**, 1087 (2008).

[13] M. S. Iovu, I. A. Cojocaru, E. P. Colomeico, Chalcogenide Lett. **4**(5), 55 (2007).

[14] T. Schweizer, B. N. Samson, J. R. Hector, W. S. Brocklesby, D. W. Hewak, D. N. Payne, Infrared Phys. Techn. **40**, 329 (1999).

[15] V. Moizan, V. Nazabal, J. Troles, P. Houizot, J. L. Adam, J. L. Doualan, R. Moncorge, F. Smektala, G. Gadret, S. Pitois, G. Canat, Opt. Mater. **31**, 39 (2008).

[16] L. Sojka, Z. Tang, D. Furniss, H. Sakr, A. Oladeji, E. Beres-Pawlik, H. Dantanarayana, E. Faber, A. B. Seddon, T. M. Benson, S. Sujecki, Opt. Mater. **36**, 1076 (2014).

[17] H. Sakr, D. Furniss, Z. Tang, L. Sojka, N. A. Moneim, E. Barney, S. Sujecki, T. M. Benson, A. B. Seddon, Opt. Express **22**, 21236 (2014).

[18] B. J. Park, H. S. Seo, J. T. Ahn, Y. G. Choi, D. Y. Jeon, W. J. Chung, J. Lumin. **128**, 1617 (2008).

[19] L. Sojka, Z. Tang, H. Zhu, E. Beres-Pawlik, D. Furniss, A. B. Seddon, T. M. Benson, S. Sujecki, Opt. Mater. Express **2**, 1632 (2012).

[20] K. Koughia, M. Munzar, D. Tonchev, C. J. Haugen, R. G. Decorby, J. N. McMullin, S. O. Kasap, J. Lumin. **112**, 92 (2005).

[21] G. Tang, C. M. Liu, Z. Y. Yang, L. Luo, W. Chen, J. Non-Cryst. Solids **355**, 1585 (2009).

[22] K. Maeda, T. Sakai, K. Sakai, T. Ikari, M. Munzar, D. Tonchev, S. O. Kasap, G. Lucovsky, J. Mater. Sci.-Mater. EL. **18**, S367 (2007).

[23] R. P. Wang, Amorphous Chalcogenides: Advances and Applications, Pan Stanford Publisher, Singapore, 170 (2014).

[24] L. Agazzi, J. D. B. Bradley, M. Dijkstra, F. Ay, G. Roelkens, R. Baets, K. Worhoff, M. Pollnau, Opt. Express **18**, 27703 (2010).

[25] S. L. Li, G. Fu, Y. K. Ye, Nucl. Instrum. Meth. B **307**, 434 (2013).

[26] A. B. Seddon, Z. Q. Tang, D. Furniss, S. Sujecki, T. M. Benson, Opt. Express **18**, 26704 (2010).

[27] E. R. Barney, Z. Q. Tang, A. Seddon, D. Furniss, S. Sujecki, T. Benson, N. Neate, D. Gianolio, Rsc Adv. **4**, 42364 (2014).

[28] F. Auzel, Chem. Rev. **104**, 139 (2004).